TOWARDS ROUTINE REAL-TIME SPACE DEBRIS MEASUREMENTS WITH EISCAT

Jussi Markkanen

EISCAT, Sodankylä, Finland, Email: jussi.markkanen@sgo.fi

ABSTRACT

In the beginning of 2005, EISCAT entered the third phase in continuing contract work for ESA. In 2005, we intend to conduct about 500 hours of measurements of space debris in LEO with the EISCAT ionospheric radars, piggy-backed on top of the standard EISCAT measurements. We use a special, workstation-based, digital receiver back-end and pulse-to-pulse coherent integration. A crucial step in achieving real-time detection speed is to use for spectrum computation a tailor-made algorithm, which boosts detection computation speed by more than a factor of 100. Our first "routine", 100-hour, real-time measurement campaign, in November 2004, found 1518 targets, with the detection sensitivity corresponding to detecting a sphere of 2 cm diameter at 1000 km range.

Key words: EISCAT; Space debris; Coherent integration.

1. INTRODUCTION

Since the early 1980's, the EISCAT mainland radars—the Tromsø UHF radar at latitude 69.6°N, operating at 930 MHz and the VHF radar operating at 225 MHz—have been performing ionospheric measurements to the order of 2000 hours per year; and since the late 1990s, after the EISCAT Svalbard radar (latitude 78.2°N) became operational, EISCAT has been measuring more than 3000 hours annually. The interest is to use a substantial amount of these operating hours for simultaneous space debris (SD) measurements in a cost-effective way. In 2000-2001, colleagues in Sodankylä Geophysical Observatory (SGO) and myself undertook an initial study for ESA on the feasibility of using the EISCAT radars for SD measurements (ESA, 1999). We demonstrated that by using a special digital receiver back-end, which we call the space debris receiver, and applying pulse-to-pulse coherent integration in the data processing, it was possible to achieve detection sensitivity corresponding the detection of 2 cm spheres at 1000 km range (Markkanen et al., 2002). The initial study showed that it was no problem to perform the SD measurements in parallel with normal EISCAT ionospheric measurements, and that a usable event rate, 10–20 targerts per hour in LEO, was achieved.

Our radar-ambiguity-function based method of pulse-to-pulse coherent integration, which we call the match function (MF) method, computes spectra of tightly sampled signals which span tens of interpulse periods, and is computationally demanding. With the MF method, in typical measurement setup, target detection in real-time requires about 100 GFlops computing speed. In the 3rd European Space Debris conference in 2001, we had to concede that with the 50 MFlops processing speed that we had achieved at the time, it would take more than a century of CPU time to analyze just one year's quota of EISCAT SD measurements. But soon afterwards, M Lehtinen from SGO, who was the project leader of the initial study, realized that by accepting some loss of detection sensitivity and a small bias in the velocity estimate, it would be possible to speed up detection computations drastically, typically by more than two orders of magnitude. We use the term fast match function algorithm (FMF) for the resulting computation scheme. The basic FMF scheme is sketched in Fig. 5.

In 2003, ESA commenced a second study with us, to bring the analysis of significant amounts of EISCAT SD data up to real-time speed (ESA, 2002). The study, finished in 2004, achieved the processing speed increase by about a factor of 10 000 (Markkanen and Postila, 2005). The FMF algorithm is about 100 times faster than the original MF algorithm, basically by managing to do with about 100 times less floating point operations per detection. A further factor of ten was obtained by coding the MF and FMF algorithms in C instead of Matlab. In addition, Apple computers have progressed from 450 MHz single-processor G4 workstations to the present-day dual-processor 2 GHz G5s, giving a further factor of ten in processing speed. The achieved speed allows real-time detection and parameter estimation to be done with a single G5 Mac.

During the second study, in four measurement campaigns, we collected and analysed about 150 hours of data, all at the EISCAT UHF radar in Tromsø. These data contain about 2500 targets. Examples of the data are shown in Fig. 6 and Fig. 7. About 500 hours of EISCAT

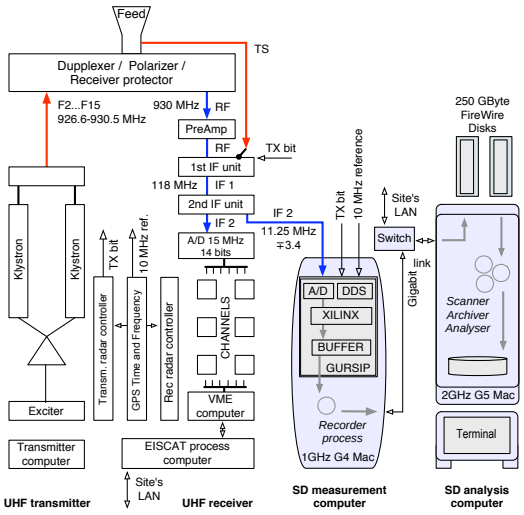

Figure 1. The space debris (SD) receiver connected to the EISCAT UHF radar. The SD receiver consists of a measurement computer and an analysis computer. The measurement computer hosts a custom signal processing board (GURSIP). The primary analog input to the SD receiver is the EISCAT second intermediate frequency (IF 2) band. The input contains, time-multiplexed, both the standard received signal and the transmission sample signal (TS). On the processing board, there is an analog-to-digital converter (A/D) taking 40 megasamples per second; a direct-digital-synthesizer chip (DDS), which provides clock signals on the board, phase-locked to the host radar's 10 MHz frequency reference signal; two Xilinks signal processing chips (XILINX) to perform signal demodulation and sampling rate reduction; and a memory buffer for temporary storage of the samples. The recorder program running on the measurement computer moves the samples over a gigibit network link to an external FireWire disk, mounted on the analysis computer. Target detection is done by the scanner program running on the analysis computer, using the FMF-algorithm. After detection, two other software modules, the archiver and the analyser, store away the event's raw data, and estimate and save the target parameters.

SD data should become available during 2005, within the third phase of the ESA-EISCAT contract (ESA, 2004).

2. MEASURING SYSTEM

To be able to use our own data processing, optimized for coherent signals, we use a special digital receiver backend, the space debris receiver. The signal to the SD receiver is branched-off from the EISCAT analog signal path at the second IF (IF2) level. Fig. 1 shows the main blocks of the SD receiver, connected to the EISCAT UHF system at the Tromsø site.

The standard EISCAT data processing handles a multi-frequency transmission by feeding the IF2 data to multiple hardware channels, each tuned to a particular center frequency. Our approach in the SD receiver is different. We sample the analog IF2 band fast enough to capture the relevant frequency channels into a single digital stream. According to the bandpass sampling theorem, we need to take B million complex samples per second, in the minimum, if the spread of frequencies is B MHz. For the most common measuring mode, where EISCAT transmits on two frequency channels, 300 kHz apart, we use 500 kHz sampling rate in the SD receiver.

In addition to the standard reception, our data processing requires the transmission waveform to be sampled. As indicated in Fig. 1, EISCAT provides the analog transmission sample signal (TS) time-multiplexed in the same data path as the reception.

The core of SD receiver is a custom PCI board which performs sampling, quadrature detection and sampling rate reduction. The board was developed originally for ionospheric tomography by the now defunct Finnish company Invers Ltd. The A/D converter on the PCI board samples at 40 MHz. The resulting real-valued sample stream is processed by programmable logic chips, from the Xilinks SpartanXL family, to perform quadrature detection, essentially by doing Hilbert transform. The result of the transform is a complex-valued sample stream at 10 MHz rate, representing the negative frequency part of the spectral contents of the analog input. The chip then decimates the 10 MHz stream to the final sampling rate. Typical decimation factor D is 20, which yields the 500 kHz final sampling rate. The decimation is done by adding samples in blocks of D; this ensures proper filtering.

The PCI board is mounted in a dual-CPU Mac G4 workstation, the measurement computer, running under Mac OS X UNIX. There is a dual-CPU Mac G5 analysis computer for target detection and parameter estimation. The two workstations are connected by a gigabit Ethernet link. The measurement computer runs software of Invers Ltd to read sample data from a buffer and write them to a hard disk, mounted over the fast link from the analysis computer. The raw data accumulation rate with the 500 kHz sampling rate is 6.7 GBytes per hour. After processing, we store permanently only about 10 seconds of raw data around each detected event, so that 10 000 events, the anticipated annual quata, requires about 200 GBytes of storage.

3. DETECTION AND PARAMETER ESTIMATION

Assume first that the received, detected signal s is just a Doppler-shifted pulse train, of M pulses of length L and interpulse period P,

$$s(t) = b_0 \left[\sum_{m=0}^{M-1} \epsilon(t - mP) \right] \mathrm{e}^{i\omega_0 t}\,, \qquad (1)$$

where $\epsilon(t)$ is unity when $t \in [0, L]$ and is zero otherwise. The signal is phase-coherent. Denote by $S(\omega)$ its Fourier-transform. The quantity $|S(\omega)|^2/(ML)$ is the power spectral density (PSD) of the signal. For any signal, the integral of the PSD, multiplied by the integration time, gives the signal's total energy E_s. For the coherent signal Eq. (1), the energy can also be found from the maximum value of the PSD,

$$\max_\omega \frac{|S(\omega)|^2}{ML} = M \cdot L|b_0|^2 = E_\mathrm{s} \tag{2}$$

According to Eq. (2), the maximum of the PSD, achieved at position $\omega = \omega_0$, increases linearly with the number of pulses included in the spectrum computation. Finding the maximum of the PSD in this way achieves pulse-to-pulse coherent integration. The time $T_\mathrm{c} = MP$ is the integration time. Coherent integration is useful in detecting a coherent signal in the presence of white noise, for the signal PSD maximum value increases with integration time, but the expectation value of the noise PSD is kT_sys, independent of the integration time (T_sys is the system noise temperature). A suitable target detection criterion is to require that the dimensionless "energy-to-noise-ratio" ENR,

$$\mathrm{ENR} = \frac{E_\mathrm{s}}{kT_\mathrm{sys}} \tag{3}$$

exceeds some predefined threshold value. In our typical measurements, we have found that we can use the threshold value of 25, without much risk of false alarms. (Or at least without much risk of false alarms due to the thermal noise; but there are other sources of disturbances, such as clutter from the ionosphere, which are more problematic in our data, see Fig. 2.) At the EISCAT UHF radar, with T_sys 100 K, transmission power 1 MW and duty cycle 10%, $\mathrm{ENR} = 25$ corresponds to the coherent echo from a 2 cm sphere at 1000 km range, integrated for 300 ms.

Another possibility to increase detection sensitivity is to compute the PSD maximum for M pulses separately and average the energy estimates. This we call non-coherent pulse-to-pulse integration. For it, we require the signal coherence only for each interpulse period separately, a much easier requirement to fulfill. For instance, acceleration correction such as used in Eq. (4) is then not needed. Nevertheless, for coherent signals the coherent integration makes better use of available information, and is expected to result in better detection sensitivity and greater parameter accuracy. To verify the fulfillment of the expectation, I have recently started to analyse our data also with non-coherent integration. Although I hope that the jury is still out, it appears that we have not gained much sensitivity from the considerable effort we have invested in the coherent integration, see Fig. 2–4.

The signal Eq. (1) is too simple as a model of the actual SD echo in EISCAT. A more realistic model takes into account that the signal arrival time (target distance) is unknown; that the Doppler-velocity cannot be taken constant when longer integrations than just a few tens of milliseconds are attempted; and that the signal typically is phase-code modulated. To be able to apply coherent integration by maximizing the PSD, the signal is first transformed to the simple form of Eq. (1). The unknown range is taken care of by trying all relevant ranges. The phase modulation is taken into account by multiplying the received signal by the measured transmission sample signal $x(t)$, this will cancel the phase flips so that the product will be of the type $\epsilon(t)$. Finally, we allow for a constant rate-of-change of the signal's Doppler-frequency during the coherent integration, by multiplying the received signal by an acceleration term $\mathrm{e}^{-i\alpha t^2}$, where α is linearly related to the radial acceleration of the target. Thus, we compute the PSD from the modified signal

$$y(t) = z(t)x(t - 2R/c)\mathrm{e}^{-\alpha t^2}\,, \tag{4}$$

where we have also acknowledged that the signal we actually have available is not s but the noisy signal $z(t) = s(t) + \gamma(t)$. The factor ML in the nominator of Eq. (2) is generalised to $\int |x(t)|^2 dt = \|x\|^2$, so that instead of maximizing $|S(\omega)|^2/(ML)$, we perform coherent integration by maximizing the "match function" MF,

$$\mathrm{MF} = \frac{|Y(\omega)|}{\|x\|} = \frac{|\int z(t)x(t - 2R/c)\mathrm{e}^{-\alpha t^2} \cdot \mathrm{e}^{-i\omega t} dt|}{\|x\|}\,. \tag{5}$$

With the measured signal $z(t)$ fixed, the MF is a function of R and α, in addition to ω. After subtracting the noise background, we use the value of the MF^2 maximum as the estimate of the signal energy,

$$\widehat{E_\mathrm{s}} = \max_{\omega,R,\alpha} \mathrm{MF}^2 - kT_\mathrm{sys}\,. \tag{6}$$

The maximum's location $(\widehat{\omega}, \widehat{R}, \widehat{\alpha})$ yields the target radial velocity and acceleration, and the target range.

The denominator in Eq. (5) can be written succinctly as the inner product $|\langle z, \chi\rangle|$, where χ is

$$\chi(R, \omega, \alpha; t) = x(t - 2R/c)\mathrm{e}^{i\alpha t^2}\mathrm{e}^{i\omega t}\,. \tag{7}$$

The MF definition in Eq. (5) becomes

$$\mathrm{MF} = \frac{|\langle z, \chi\rangle|}{\|\chi\|}\,. \tag{8}$$

The parametrized functions χ represent possible received signals, and are referred to as the model functions. We can rephrase the MF method of parameter estimation as the task of finding the best-matching model function among the set of all model functions, in the precise sense of maximizing the match function $\mathrm{MF}(R, \omega, \alpha)$. The expression Eq. (8), or some near relative, is often called the radar ambiguity function in the literature.

The MF is in practice evaluated based on the sampled data vector $z_n = z(n\tau_\mathrm{s})$ and similarly sampled noise data γ_n. We discretize the ω variable in such a way that we can use FFT in evaluating the Fourier-transform $Y(\omega)$ in Eq. (5). In detection, FFT of a data vector of the length on the order of 100 000 points needs to be computed for each

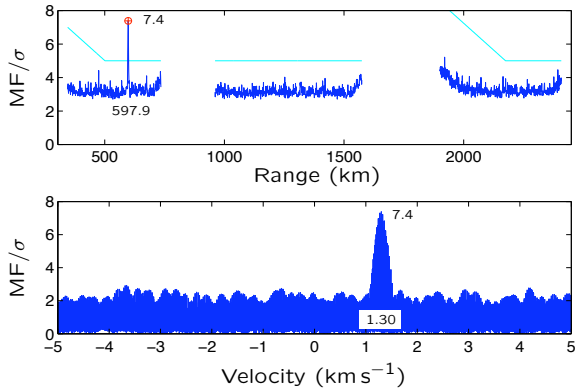

Figure 2. Detection with the MF *algorithm. Data is from EISCAT tau2 experiment, 12-Nov-2005. Sampling interval 2 μs, coherent integration 312 ms. 2^{18} point FFT was used to compute the MF velocity slice (power spectrum) $v \mapsto \mathrm{MF}(\widehat{R}, v)$ shown in the bottom panel. The 25×10^6 operation computation required 44 ms on a 2 GHz Mac G5 workstation. To compute all the 1685 range gates R of the curve $R \mapsto \max_\omega \mathrm{MF}(R, \omega)/\sigma$, shown in the top panel, took 75 s. A target is detected at range $\widehat{R} = 597.9$ km, velocity 1.3 $\mathrm{km\,s^{-1}}$, with energy-to-noise ratio 7.4^2. An effective diameter of 1.7 cm was determined for this target.*

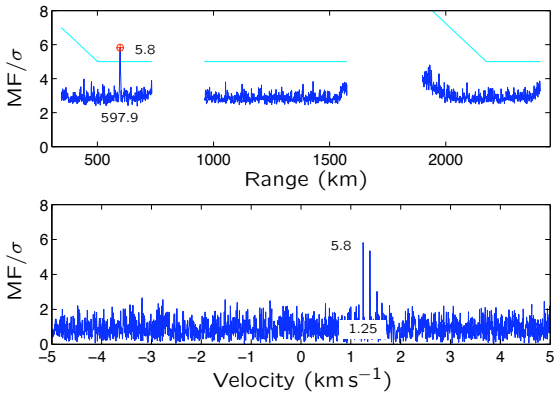

Figure 3. Detection with the FMF *algorithm. A 2^{12} point FFT was used for power spectrum computation, resulting in more than 7 GFlops speed in the FFT itself. The other operations involved in the* FMF *are slower, but the mean performance was still about 2 GFlops. It took 0.23 ms to compute the spectrum, and 0.41 s to go through all the 1685 ranges. The target range and velocity determined from the FMF maximum location are not much different from those given by the MF algorithm; the maximum value has dropped from 7.4 to 5.8.*

of the typically 2000 range gates R_j, and then the maximum found according to Eq. (6). We should also vary the acceleration parameter α, but so far we have taken α to be a fixed, predetermined function of range, $\alpha = \alpha(R)$, computed by assuming that the target is on a circular orbit and the antenna is pointed vertically. Even then, the straightforward detection computation comes too large for a real-time application. Fig. 2 shows a typical example, where it took 75 seconds to handle 0.31 seconds of raw data on a G5 Mac.

The detection computation time can be reduced by more than a factor of 100 by making use of special properties of our measuring configuration in EISCAT, namely, that we are using pulsed transmission with about 10% duty cycle, so that most of the vector to be Fourier-transformed is known to be zero, and also that the raw data is heavily oversampled with respect to the expected target Doppler-shifts. The FMF algorithm, sketched in Fig. 5, makes use of these properties to reduce the length of the vector to be actually Fourier-transformed by a factor of about 100. There is a penalty in terms of detection sensitivity, but in practice the penalty is tolerable. Fig. 3 shows the same raw data vector as in Fig. 2, now handled with the FMF algorithm. The time required to handle the 0.31 s of raw data has gone down from 74 s to 0.41 s. The latter time actually already is sufficiently small for detection to keep up with the incoming data flow, for we normally can skip some data, say about 0.2 s in this case, between the integrations.

We estimate the final target parameters (range, velocity, effective diameter) by re-scanning the event's raw data with maximal spatial and temporal resolution. For most targets, the target's beam passage results in time series of range, velocity and energy-to-noise ratio; the final parameters we tabulate are fitted from the time series for the time instant of maximum signal strength.

4. DATA

We performed our longest SD measuring campaign to date from 09:02 UT, November 9th, to 14:00 UT, November 13th during a standard EISCAT "common mode" CP1 ionospheric experiment at the Tromsø UHF radar. The EISCAT transmission was the so called tau2 transmission. The transmission alternates between the frequencies 930.2 and 929.9 MHz, with an interpulse period of 5580 μs. In each IPP, the transmission is a 576 μs pulse, binary phase coded with a 16-bit, baud length 36 μs code. The full set of codes used has 32 codes. The transmission peak power was about 1 MHW during the campaign and the system temperature about 120 K. The UHF antenna was kept pointed along the magnetic field direction, azimuth 184.0°, elevation 77.1°. We used 2 μs sampling interval in the SD receiver, and performed the target detection search with the FMF algorithm, over the range intervals 354–735 km and 960–1575 km, using 1.5 km gate separation; these are the lowest two intervals shown in the top panels of Fig. 2–4. We noticed only afterwards, when we had already disregarded most of the raw data, and could no more re-analyze the data, that it would be useful to extend the range coverage, and added a third interval as shown in Fig. 2–4. We used detection threshold

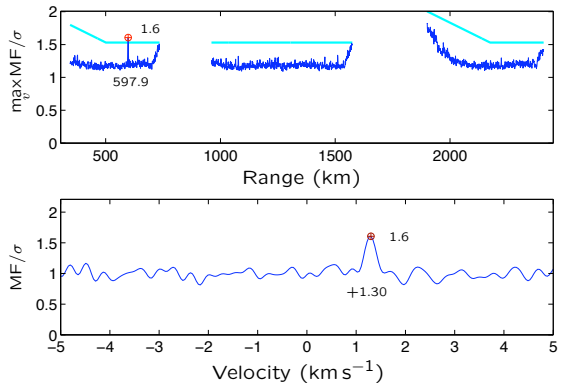

Figure 4. Detection with non-coherent pulse-to-pulse integration. The 56 IPPs long data segment was processed IPP per IPP by computing the MF*, and the squares of the individual MFs averaged. The figure shows the averaged* MF*. The sensitivity corresponds roughly to the sensitivity of the FMF, but the computation time was about 10 times longer.*

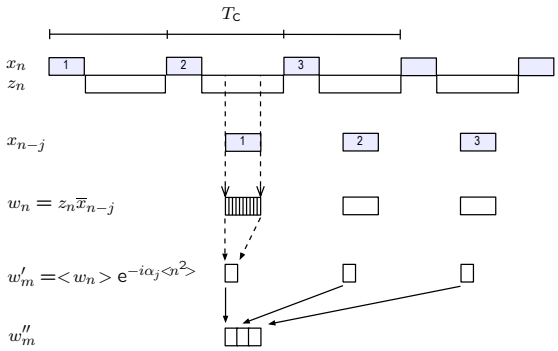

Figure 5. The FMF algorithm. For each of M transmitted pulses included in the coherent integration (M=3 in the figure), one first forms the point-wise product w of the reception z and the shifted, complex-conjugated transmission $\overline{x}$. Next, for each pulse, w is decimated by adding neighboring samples, and the decimated vector multiplied by an appropriate mean acceleration correction factor to get the vector w'. Finally, the M vectors w' are simply concatenated to form the FFT input vector w'' for the power spectrum estimate.

$\mathrm{ENR} = 5.0^2$ from the range 500 km upwards, and a ramp declining from $\mathrm{ENR} = 8.0^2$ at 375 km to $\mathrm{ENR} = 5.0^2$ at 500 km. The ionosphere is often very visible in our data (that is what the EISCAT radars and transmissions are designed for), appearing as strong clutter in SD measurements below about 500 km range and its range aliases. It is necessary to use range-dependent detection threshold in order not to waste detection sensitivity.

In the November campaign, our software allowed the raw data collection and target detection to proceed on-line, automatically and without hickups. The final event selection and parameter estimation still involved some manual work. Timewise, the software can handle also these phases in real-time, but the event selection algorithm cannot handle reliably problems due to the non-thermal irregularities in the data. We got 1518 events, plotted in Fig. 6.[1] The top panel shows the effective diameter of the targets, as based on the measured ENR and range, and the known radar parameters. The effective diameter is the diameter of the conducting sphere that would cause the observed ENR if placed at the measured range in the center of the antenna beam. Most of the targets will not actually be in the center of the beam (the half power beam width at UHF is 0.6°), but in EISCAT, it is not possible to determine the target's position within the beam, and therefore only a lower bound of the target's radar cross section, and the effective diameter, can be deduced.

The effective diameters plotted in Fig. 6 are deduced from the ENR estimated using 300 ms, FMF-based, coherent integration. However, it seems that the coherent integration efficiency is already considerably reduced from 100% at this integration time. It is not evident to me how to best estimate quantitatively the efficiency of the coherent integration (nor of the non-coherent integration).

[1]These data are available via http://www.sgo.fi/ jussi/spade/.

Simulations indicate that unless the signal is strong, or the integration time is long, even for a fully coherent signal the ENR estimate is biased so that the apparent value is too large. This leads to too *large* effective diameters. On the other hand, the assumed signal models usually will tend to be the more incorrect the longer the integration time. This effect tends to produce too *small* effective diameters.

In the ideal case, the measured ENR should increase linearly with the integration time. What happens with the actual data is shown in Fig. 8. I re-analysed a data set of about 400 events, originally detected and analysed with 300 ms integration, using 17 integration times from 45 ms to 670 ms. For each target, its vector of 17 ENR values was normalized to unity at 89 ms integration time. The large dots in Fig. 8 give the mean of the normalized vectors. For short integration times, the mean vector displays some of the expected trends, namely, the ENR increases roughly linearly, and also, appears to have a positive bias for the very shortest integrations. But then the ENR estimate rapidly saturates at about 200 ms, and starts slowly to decrease.

One way how the coherent integration can fail in such a sudden manner is if the radial acceleration that we assume in the FMF computation is not correct, but has an error Δa. The set of the closely spaced curves in Fig. 8 gives the theoretically expected ENR when Δa is 7 $\mathrm{m\,s^{-2}}$. The different curves correspond to different values of the assumed velocity error Δv. A wrong, fixed value of the acceleration will be partly compensated in the MF maximization by a slightly wrong velocity parameter. For instance, the thick curve in the figure, peaking at about 200 ms, corresponds to the velocity parameter error $\Delta v = -\Delta a T_c/2$. This Δv makes the mean

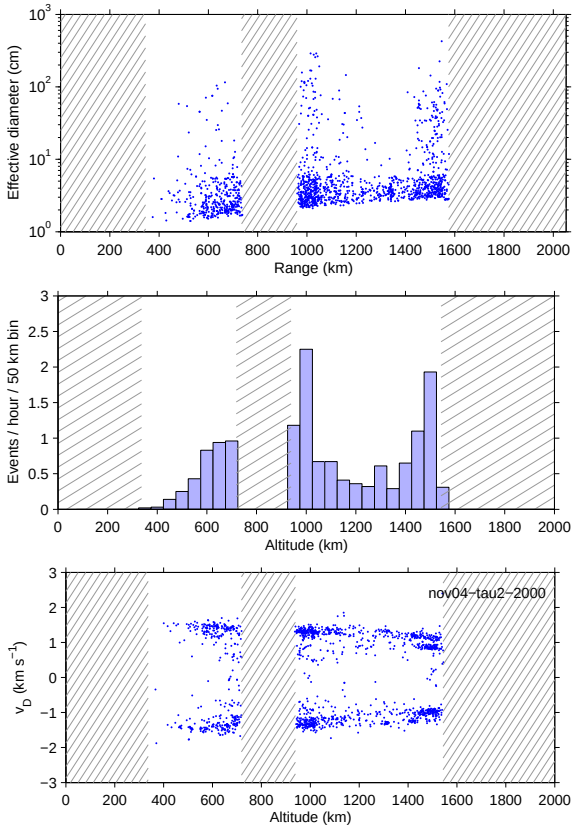

Figure 6. Data from 100 h measurement campaign at EISCAT Tromsø in November 2004. The EISCAT-experiment was tau2, which is a standard "general-purpose" experiment for ionospheric studies between about 80 and 800 km range. For SD detection, we used the next higher range windows also. Antenna was pointed to azimuth 181°, elevation 77°. Altogether 1518 analysable events were identified, with the detector set to tricker on a 2 cm diameter target at 1000 km range.

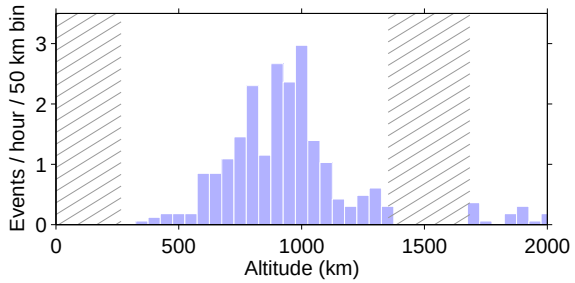

Figure 7. Detection rate as function of altitude in EISCAT's 16 hour participation to the 2004 "beam park" SD measurement, 7th September 2004. The experiment was EISCAT's long-range standard experiment, tau1, which does not have a blind spot around 800 km as tau2 does. The antenna was pointed to azimuth 133°, elevation 62°. 364 targets were detected in the altitude interval shown in this plot. The data were processed with the FMF algorithm.

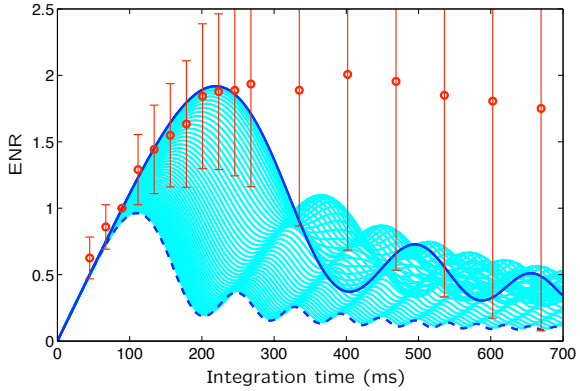

Figure 8. Loss of coherent integration efficiency due to wrong acceleration value in the signal model. The data points (dots) are from a 16 hour "beam park" measurement at EISCAT UHF radar in September 2004. The curves are theoretical shapes of MF^2*, computed assuming the fixed difference* $\Delta a = 7\ \mathrm{m\,s^{-2}}$ *between the actual target radial acceleration and the model signal acceleration, and various values of the radial velocity difference.*

velocity of the model signal to be correct during the integration. The dashed curve in the figure corresponds using the correct target velocity. The other curves represent intermediate situations. The figure suggests that it is indeed possible that an acceleration error contributes to the sudden loss of integration efficiency. On the other hand, the persistently high values of the observed ENR at long integrations are not explained by this model.

REFERENCES

ESA Directorate of Technical and Operational Support ESOC Ground Segment Engineering Department Mission Analysis Section. Study specification, measurements of small-size debris with backscatter of radio waves. Darmstadt, Germany, 1999.

ESA Directorate of Technical and Operational Support ESOC Ground Segment Engineering Department Mission Analysis Section. Study specification, real-time space debris detection with EISCAT radar facilities. Darmstadt, Germany, 2002.

ESA Directorate of Technical and Operational Support ESOC Ground Segment Engineering Department Mission Analysis Section. Study specification, small-size space debris data collection with EISCAT radar facilities. Darmstadt, Germany, 2004.

Markkanen, J., Lehtinen, M., Huuskonen A., Väänänen, A. Measurements of Small-Size Debris with Backscatter of Radio Waves, Final Report, ESOC Contract No. 13945/99/D/CD, 2002.

Markkanen, J., Postila, M. Real-Time Small-Size Space Debris Detection with EISCAT Radar Facilities, Final Report, ESOC Contract No. 16646/02/D/HK(CS), 2005.